

Original Article

Cite this article: Li C, Liu J, Ma J, Su G, Lan J, Li X, Ren Z, and Ran H (2022) Field observations of surface ruptures accompanying a tsunami and supershear earthquake along a plate boundary strike-slip fault. *Geological Magazine* 159: 893–903. <https://doi.org/10.1017/S0016756822000012>

Received: 7 May 2021

Revised: 31 December 2021

Accepted: 1 January 2022

First published online: 11 February 2022


Keywords:

Palu Mw 7.5 earthquake; strike-slip earthquake; subduction zone; destructive tsunami; supershear rupture

Author for correspondence:

Chuanyou Li,
Email: chuanyou@ies.ac.cn

Field observations of surface ruptures accompanying a tsunami and supershear earthquake along a plate boundary strike-slip fault

Chuanyou Li¹ , Jinrui Liu², Jun Ma², Gang Su³, Jian Lan², Xinnan Li^{1,4}, Zhikun Ren² and Hongliu Ran²

¹State Key Laboratory of Earthquake Dynamics, Institute of Geology, China Earthquake Administration, Beijing, China; ²Institute of Geology, China Earthquake Administration, Beijing, China; ³China Earthquake Disaster Prevention Center, Beijing, China and ⁴Earth Observatory of Singapore, Nanyang Technological University, Singapore

Abstract

Strike-slip earthquakes near major subduction zones have received less attention than thrust or reverse earthquakes in subduction zone areas. The occurrence of the 2018 Palu Mw 7.5 earthquake in eastern Indonesia provides an unprecedented opportunity to investigate the characteristics of one of these events. The Palu earthquake occurred on the left-lateral, north–south-striking Palu–Koro fault, which is the main plate boundary structure accommodating the convergence between blocks in a triple junction area. It excited a significant tsunami, which unusually is associated with strike-slip earthquakes, and also ruptured at a supershear speed, which is mostly observed on strike-slip faults in continents. Based on our fieldwork, we speculate that the normal slip component of the offshore rupture section in Palu bay on the middle segment probably favours tsunami genesis. Our field investigation has revealed evidence of a simple geometry as well as slip partitioning of dip-slip and strike-slip motion on two subparallel strands on the main segment, both of which may have contributed to the supershear of the rupture propagation. Instead of only a transtensive behaviour of the middle segment, our results also illustrate the transpressional property of the northern and southern rupture segments, which shows more complex behaviour than that of a common continental strike-slip fault.

1. Introduction

Most of Earth's largest earthquakes occur in subduction zones that constitute the most active plate boundaries and are usually densely populated. Thrust or reverse earthquakes take place more frequently than other types of tectonic events at the convergent plate boundaries. Earthquakes of this type are responsible for most of the recent loss of life and property through natural disasters in such regions, and therefore have attracted considerable attention since the 2004 Sumatra–Andaman Mw 9.0 earthquake (e.g. Ammon *et al.* 2005; Titov *et al.* 2005; Vigny *et al.* 2005; Subarya *et al.* 2006; Banerjee *et al.* 2007). Similar to thrust earthquakes, strike-slip events also pose a seismic and tsunami threat to subduction zone areas, but little is known about the rupture structures associated with them. The strike-slip faulting along a plate boundary structure during the Palu Mw 7.5 earthquake on 28 September 2018 provides an unusual opportunity to investigate the characteristics of these events.

The focal mechanism solutions and observations from geodetic, seismic and geological data (Bao *et al.* 2019; Fang *et al.* 2019; Socquet *et al.* 2019; Zhang *et al.* 2019; Wu *et al.* 2020) indicate that the earthquake occurred on the left-lateral, north–south-striking Palu–Koro fault, a main plate boundary structure that connects to the Minahassa subduction zone to the north, and accommodates the relative motion between the Makassar block and the North Sula block (Fig. 1a). One remarkable feature of the 2018 event is that this strike-slip earthquake caused an unexpected destructive tsunami (Heidarzadeh *et al.* 2019; Omira *et al.* 2019; Ulrich *et al.* 2019). Tsunamis usually accompany earthquakes that occur on thrust or reverse faults in subduction zones, but not for such an earthquake type (Prasetya *et al.* 2001; Carvajal *et al.* 2018; Mikami *et al.* 2019). Another striking feature of the 2018 event, suggested by seismic and space geodesy observations, is that the rupture propagated at supershear speeds on most of the rupture segments (Bao *et al.* 2019; Socquet *et al.* 2019), something which commonly occurs on faults with simple geometry (Bouchon & Vallée 2003; Vallée *et al.* 2008; Bouchon *et al.* 2010; Konca *et al.* 2010). Our previous study reported the primary features of the coseismic surface ruptures associated with the earthquake (e.g. coseismic slip sense, the coseismic displacement

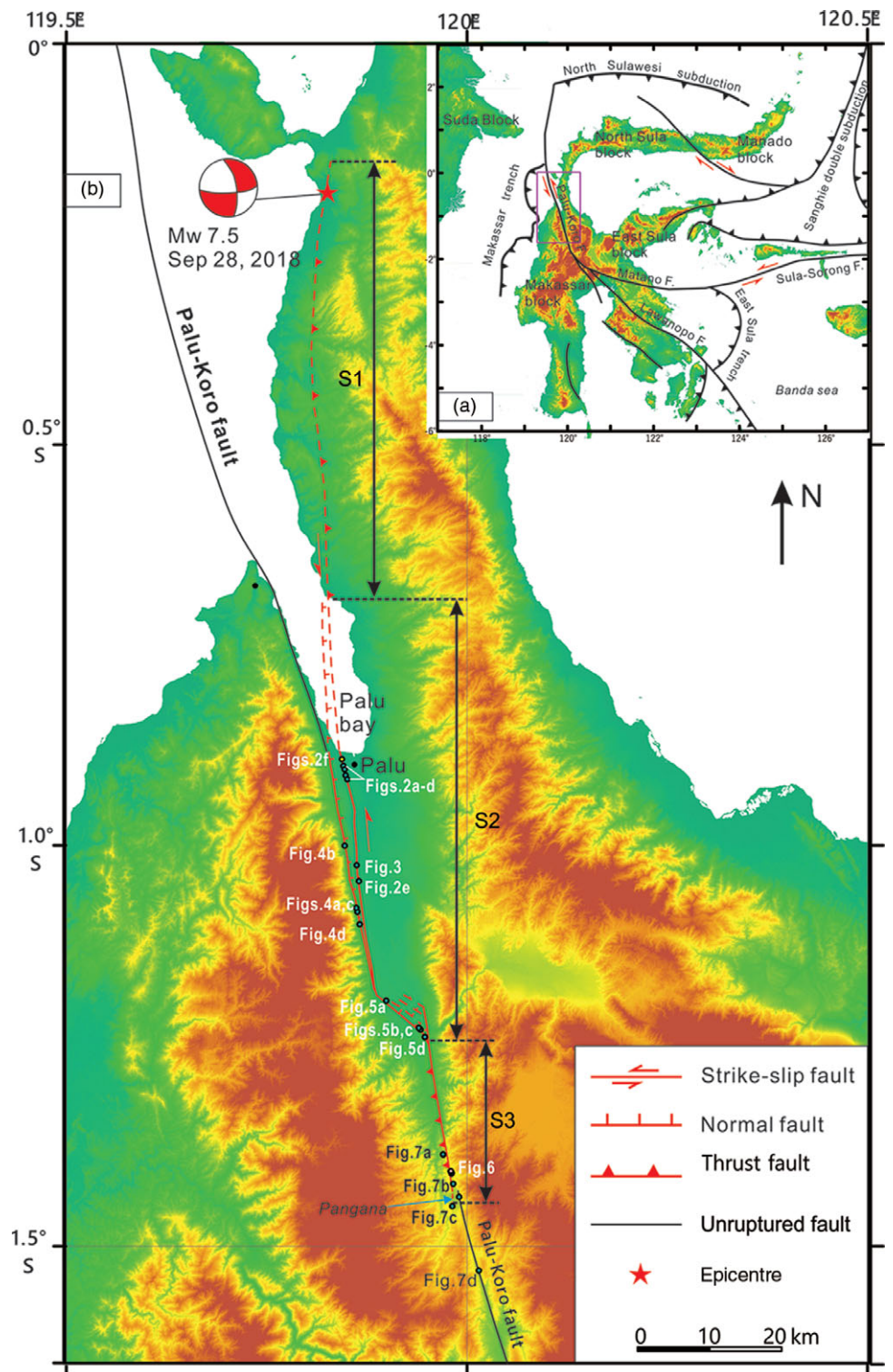


Fig. 1. (Colour online) Tectonic setting and surface ruptures associated with the Mw 7.5 Palu earthquake. (a) The island of Sulawesi, where the 28 September 2018 Mw 7.5 earthquake occurred, is located at the junction of several blocks. The Palu-Koro fault, which produced the 2018 earthquake, is the main plate boundary structure in the Sulawesi area. (b) The extent of the surface ruptures of the 2018 Palu earthquake. Solid red lines: rupture sections mapped in the field; dashed red lines: rupture sections suggested by interferometric synthetic aperture radar (InSAR) and seismic studies (e.g. Bao *et al.* 2019; Fang *et al.* 2019; Socquet *et al.* 2019). S1-S3: northern, middle and southern segments, respectively. Note that the middle segment of the rupture zone consists of two strands. The geological traces of the unruptured faults are shown in black. The epicentre is indicated by a red star. The epicentre and the focal mechanism are from US Geological Survey (2018).

distribution, the seismogenic fault), based on a limited number of field investigations carried out immediately after the earthquake (Wu *et al.* 2020). However, that previous study is preliminary, and the assessment of the fault geometry, the identification of rupture segments, and details of the fault's seismotectonic behaviour remain unclear because of a lack of detailed field investigations, which are important for understanding rupture propagation and termination and assessing the kinematics, rupturing process and

the seismic hazard of an interplate strike-slip fault. In this study, a thorough investigation and detailed mapping of the coseismic surface rupture structures in the field allowed us to understand what may have caused the puzzling tsunami and further discuss the role of rupture geometry in a supershear event.

To better understand the characteristics of the surface ruptures and related faulting behaviour of such a strike-slip earthquake at convergent plate boundaries, we carried out additional detailed

field investigations along the surface ruptures of the 2018 Palu earthquake three and a half months after the earthquake. Based on the previous fieldwork, we investigated geometric and geomorphic features of the surface rupture in greater detail, and discuss the rupture mechanism of a supershear interplate earthquake.

2. Tectonic setting

The Palu–Koro fault and its southeast continuation (the Matano fault) are the main active structures in Sulawesi, eastern Indonesia, a triple junction where the Australian, Philippine Sea, Pacific and Sunda plates (eastern part of Eurasia) meet (Walpersdorf *et al.* 1998a; Socquet *et al.* 2006). The Palu–Koro fault obliquely crosses the Sulawesi island and divides it into two parts: the Sula block to the northeast and the Makassar block to the southwest (Fig. 1a). The crustal blocks' relative motion accommodates the convergence between the plates in the junction area (Fitch 1972; Silver *et al.* 1983; Walpersdorf *et al.* 1998a; Stevens *et al.* 1999; Kreemer *et al.* 2000; Vigny *et al.* 2002; Socquet *et al.* 2006). Sinistral transpression through the Sula–Sorong fault in the east is transformed by left-lateral strike-slip along the Matano fault and the Palu–Koro fault to the west and the north, then absorbed at the Minahassa Trench, where the Sunda plate subducts southward beneath the Sula block (e.g. Hamilton 1979; Silver *et al.* 1983; Rangin *et al.* 1999) (Fig. 1a).

The ~300 km long, left-lateral Palu–Koro fault connects the north Sulawesi subduction zone in the north and shows a transforming behaviour. Much of its trace north of the Palu gulf is under water, and runs through the 2018 epicentral area. To the south, the fault trace is well expressed in the Palu valley, and becomes more linear southward. In addition to evidence for late Quaternary geomorphic features associated with strike-slip faulting, the major fault bounding the Palu valley is marked by faceted escarpments including a several metres high scarp, which suggests that the recent motion of the fault contains a substantial normal component (e.g. Bellier *et al.* 2006). Slip on the Palu–Koro fault accommodates rotation of the Sula block at a rate of between ~35 mm a⁻¹ determined by geological studies (Bellier *et al.* 2001) and ~42 mm a⁻¹ inferred from GPS (the global positioning system) observation (Walpersdorf *et al.* 1998b; Stevens *et al.* 1999; Socquet *et al.* 2006). Estimates from plate kinematics and palaeomagnetic studies suggest a similarly high slip rate of ~30–50 mm a⁻¹ across the fault (Silver *et al.* 1983; Surmont *et al.* 1994). According to the empirical relations between displacement and magnitude for strike-slip earthquakes, the recurrence interval for magnitude $M > 7$ earthquakes on the Palu–Koro fault is ~100 years if it slips at a rate of 40 mm a⁻¹ (Socquet *et al.* 2006). The characteristic earthquake model and such a recurrence interval can account for the low seismicity in the past 100 years.

3. Observations

Both seismic inversion results (Bao *et al.* 2019; Zhang *et al.* 2019; Li *et al.* 2020) and geodetic observations (Fang *et al.* 2019; Socquet *et al.* 2019) suggest the rupture of the 2018 Palu M_w 7.5 earthquake nucleated near the epicentre located ~80 km north of the city of Palu, and propagated mainly unilaterally southward along the Palu–Koro fault for ~150 km. The coseismic slip was mainly left-lateral strike-slip with some vertical component. Based on our field investigation, combined with knowledge of previous studies from seismic and geodetic observations, the 2018 earthquake rupture zone can be divided into three segments: the northern,

the middle and the southern (Fig. 1b), separated by bends or steps identified in our work and previous studies (Fang *et al.* 2019; Socquet *et al.* 2019).

3.a. The northern segment

The northern segment of the 2018 rupture did not follow the previously mapped trace offshore, but broke on land within the Sulawesi neck (Fig. 1b). This segment is constrained based mainly on seismic and geodetic studies (Fang *et al.* 2019; Socquet *et al.* 2019), due to the extraordinary difficulty of carrying out field investigation in such a remote, mountainous area and the fact that there is almost no way to gain access to the fault. The rupture exhibits a much-smoothed displacement gradient, which indicates that along this segment the fault probably did not break the surface. A coseismic lateral slip of up to ~2 m was measured by geodetic studies (Fang *et al.* 2019). Uplift occurred to the east of the fault (Socquet *et al.* 2019), which suggests a thrust slip component on this segment, especially in the area of the northern portion close to the epicentre. The maximum thrust slip observed around 0.35° S on this segment is also ~2 m (Fang *et al.* 2019). The rupture trace along this segment is less straight than it appears along the southern segments and propagated southwards for ~60 km before reaching Palu bay.

At ~0.7° S, the rupture entered offshore and propagated southward for ~21 km within Palu bay. Around the part between 0.7° S and 0.8° S, the fault behaves transpressionally, displaying comparable strike-slip with dip-slip components (Fang *et al.* 2019). Therefore, this point (~0.7° S) acts as a boundary between the northern and middle segments.

3.b. The middle segment

Significant normal-slip components are observed in the offshore part to the south. Along this portion within Palu bay, left-lateral strike-slip of up to 6 m with normal slip of up to 2 m was observed geodetically (Ulrich *et al.* 2019). The coseismic rupture section south of Palu bay is the main surface rupture of the 2018 event and shows a very sharp trace both in field and in satellite images. By combining field studies with analysis of satellite images acquired after the earthquake, we mapped the surface rupture in detail. In the middle segment, the 2018 earthquake broke two distinct subparallel strands, 1–1.3 km apart: a strike-slip strand in the east and a normal strand in the west (Fig. 1b). A similar phenomenon was also identified geodetically (Socquet *et al.* 2019). The ruptures propagated from the bay, then extended southward on land, which suggests that similar fault geometry possibly occurred offshore in the bay and the on-land segment is a continuation of the offshore extent. This point is also supported by the similar motion and slip magnitude on both sections. From a geomorphic perspective, Palu bay and the Palu valley seem to belong to a NWN-striking rift caused by the pull-apart structure in the Palu area. The eastern strand traverses a flat, alluvial floodplain on which Palu city is situated, and exhibits almost pure strike-slip motion along the main stretch of this rupture strand. This strand is located up to 1.5 km east of the mapped fault trace and does not appear to lie on pre-existing scarps along a large portion of the fault. From the southern shoreline of Palu bay to the southern end of this segment, the strike-slip strand is mostly simple, narrow and continuous (Fig. 2; Figs S2 and S3 in the Supplementary Material available online at <https://doi.org/10.1017/S0016756822000012>). The rupture generally displays as a zone consisting of multiple subparallel fault strands with a width varying from several metres to tens of



Fig. 2. (Colour online) Coseismic left-lateral slip along the middle segment of the 2018 surface rupture zone. (a) Offsets of a street and a small canal near Jl Asam II in Palu city, with sinistral displacement of $c. 3.0 \pm 0.2$ m, view to the east; (b), another site in Palu city showing typical strike-slip offsets of the 2018 surface rupture zone (west view), sinistral displacement of $\sim 4.2 \pm 0.2$ m; (c, d) surface breaks exhibiting as a ~ 5 – 10 m wide zone constituted by several parallel strands (indicated by light purple arrows and dark purple arrows), views to the west and east, respectively; (e) coseismic left lateral offsets of the field edges south of Palu city, view to the south. (f) An oblique UAV image showing the coseismic surface rupture at the site where the maximum coseismic left-lateral offset was measured in the previous study (Wu *et al.* 2020). The red arrows show the locations and strike of the fault trace, the yellow arrows indicate the offset features. See Figure 1 for locations.

metres (Fig. 2c and d). It is also displayed as a ~ 1 m wide opening with left-lateral slip (Fig. 3a; Fig. S3f in the Supplementary Material available online at <https://doi.org/10.1017/S0016756822000012>) or defined as a series of NWN-striking, right-stepping en echelon tension fissures in some places. Coseismic offsets were measured across linear surface landmark features that cross the fault, such as roads, fences, walls, canals, crop rows, ditches, treelines and field boundaries (Fig. 2). Most of the offset features we selected to measure are nearly perpendicular to the fault strike; azimuthal corrections can be neglected. To the features not strictly perpendicular to the fault, the pierce points of the offset markers have been projected on a vertical plane striking perpendicularly to the fault trace; such azimuthal corrections can ensure a reliable value of the offset amounts. The left-lateral slips are commonly 3–5 m, with a maximum value of 5.5 ± 0.1 m measured at the site (1.025° S) near Mesjid Alkhairaat, 15 km south of Palu bay, based on offset of field boundaries

(Fig. 3). The maximum coseismic horizontal displacement is obtained from measurements both in the field and on the unmanned aerial vehicle (UAV) images. The maximum coseismic offset was previously reported to be ~ 6.2 m by our group, based on a preliminary result during the first field investigation, a value obtained only from the UAV image of an offset vehicle track (Fig. 2f). We re-examined that rupture section and found that surface ruptures at that site have a complicated pattern, which makes the accurate matching of offset piercing lines difficult. Measurements of several offset linear geomorphic markers across this fault section yield the coseismic horizontal displacements from 2 to 4 m, which suggest the coseismic lateral slip should be in the range 2–4 m along this section. Thus, we infer that the maximum offset of 6.2 m was somewhat misinterpreted.

The western strand runs at the base of the sharp range front west of the Palu valley, with prominent triangular facets several

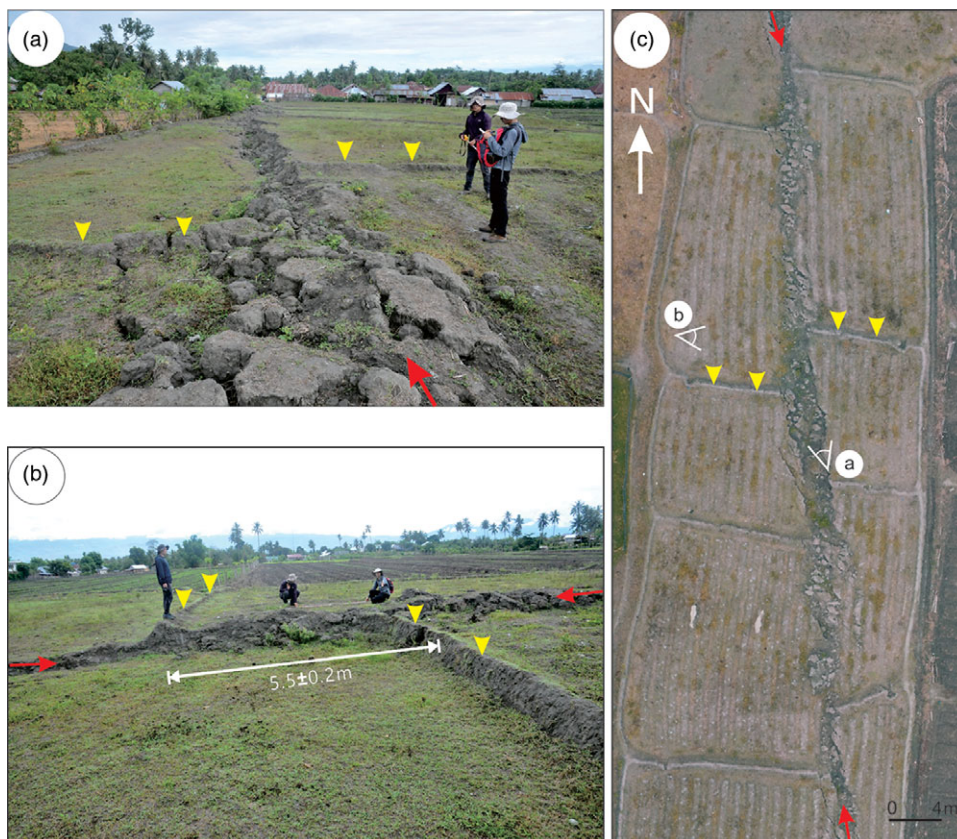


Fig. 3. (Colour online) Photos and UAV image showing maximum coseismic left-lateral slip along the middle segment of the 2018 surface rupture zone. (a) Surface break exhibiting as a 1–2 m wide crack with ~5 m sinistral displacement (north view, see the location in (c)); (b) the maximum strike-slip displacement observed in the field (east view, see the location in (c)); (c) an oblique UAV image of a surface rupture section. The red arrows show the locations and strike of the fault trace; the field edges are indicated by the yellow arrows. See Figure 1 for locations.

hundred metres high (Fig. 4a; see Supplementary Material for more figures). The surface break is discontinuous, and consists of open cracks and small scarps showing mainly normal faulting with a vertical, down-to-the-east offset of generally 30–150 cm (Fig. 4 b–d). Along this normal strand, the surface rupture closely follows the previously mapped fault trace. Fresh opening is usually observed at the base of a pre-existing escarpment (Fig. 4c–d; Fig. S4b–d in the Supplementary Material available online at <https://doi.org/10.1017/S0016756822000012>). Continuous ground cracking ~5 km long has been mapped along the mountain front in the central part of this rupture strand, following a pre-existing fault trace defined by scarps and lineaments. In other areas, surface ruptures are generally discontinuous and short, especially approaching the southern end. The two rupture strands run alongside each other for *c.* 35 km on land before they merge into a single rupture zone at the southern limit of the Palu valley. The junction is characterized by a bend where the azimuth of the strike rotates by ~20° counterclockwise, which could be considered as a segment boundary (Fig. 1b). Within this ~8 km long extensional bend, faulting is distributed throughout a 1 km wide zone of surface cracking, each crack showing several to tens of centimetres of vertical displacement (Fig. 5; Fig. S5 in the Supplementary Material available online at <https://doi.org/10.1017/S0016756822000012>).

3.c. The southern segment

South of the bend, the rupture bends back to a strike similar to the overall orientation of the Palu–Koro fault (Fig. 1), and coseismic slip decreases rapidly, as indicated by discontinuous, small scarps along the fault. Then the rupture zone enters a narrow valley between high mountains, where the surface ruptures are obscured by active drainage, vegetation, landslides and steep topography.

Although observations along much of the stretch of this segment are limited because of the mountainous environment, the characteristics of the rupture are still clearly exhibited. The 2018 rupture zone along the southern segment is mostly single-stranded, and displays a left-lateral slip with a minor vertical motion (Figs 1b and 6). In contrast to the middle segment, a clear reverse component has been identified along this segment, with a vertical displacement as large as 0.4 m (Fig. 6b and c; Fig. S6a–c in the Supplementary Material available online at <https://doi.org/10.1017/S0016756822000012>). The ratio between average horizontal displacement and reverse slip is about 1:1 along the southern segment (Fig. 7b; Fig. S6a in the Supplementary Material available online at <https://doi.org/10.1017/S0016756822000012>). The surface rupture accompanying the 2018 earthquake follows pre-existing 1–2 m high scarps along the southernmost section (Fig. 6b). Slip along this segment is typically low, with a maximum observed left-lateral and vertical displacement of *c.* 50 cm and 40 cm, respectively. The rupture on the southern segment was arrested by the ~1.2-km wide Pangana basin, which acted as a step-over (Fig. 1b). Around the southern end, the rupture is characterized by a series of 10–30 cm wide extensional fissures (Fig. 7c). Based on the absence of surface breaks south of the step-over (Fig. 7d; Fig. S6d–f in the Supplementary Material available online at <https://doi.org/10.1017/S0016756822000012>), we conclude that the coseismic surface rupture of the 2018 event did not extend onto the fault segment in the south.

4. Discussion

Our field investigation, combined with previous studies on the surface ruptures of the 2018 Mw 7.5 earthquake, reveals that the

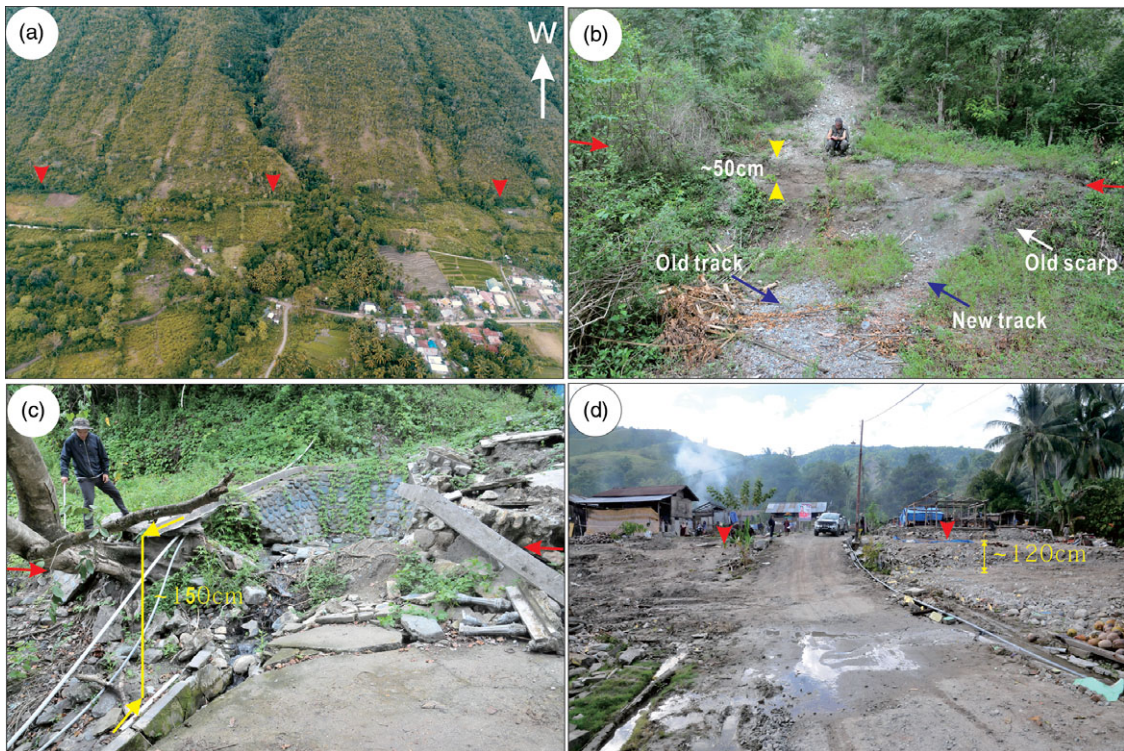


Fig. 4. (Colour online) Geomorphic expression and typical surface breaks of the 2018 earthquake along the western strand bounding the western edge of the Palu valley. (a) An oblique UAV image showing morphology by the active fault in front of the triangular facets on the Palu-Koro fault north of Buper Vatujulai; (b) west view of 2018 break with a down-to-the-east throw of 50 cm, following a pre-existing fault scarp (note that the 'new track' is a track created after the earthquake because the old one did not work due to the wide crack); (c) a canal was vertically offset ~150 cm during the earthquake and formed a small waterfall (view is to the west); (d) west view of a 120 cm high scarp formed during the 2018 earthquake. Red arrows show the locations of the fault trace and the fault scarps; the scarp heights are also shown. Locations are shown in Figure 1.



Fig. 5. (Colour online) Coseismic deformation and related tectonic geomorphology along the bend between the middle and southern segments. (a) North view of the new vertical offset superimposed on a pre-existing fault scarp around Masjid Nurul Hidayah; (b) a fence was vertically offset ~50 cm during the earthquake and formed a small scarp northeast of Mushollah (view is to the southwest); (c) the road was also vertically offset the same amount during the earthquake (view is to the south); (d) a more than 200 m long rupture with a ~20 cm high scarp observed across the farmland (view is to the east). Red arrows show the locations of the fault trace and the fault scarps. Locations are shown in Figure 1.

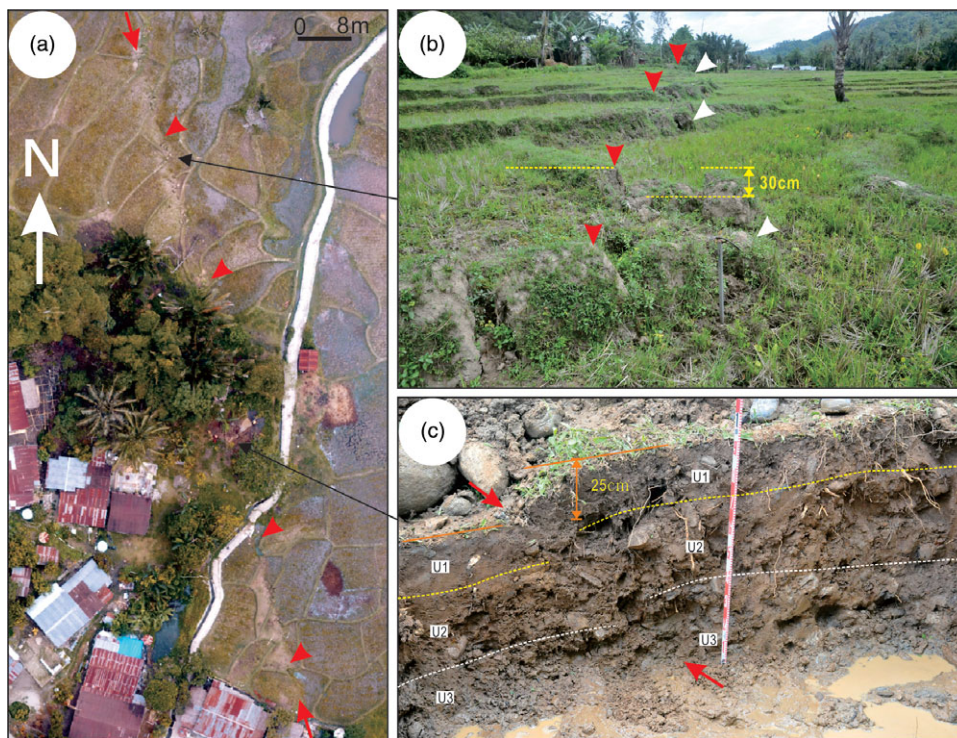


Fig. 6. (Colour online) Coseismic deformation along the southern segment of the surface rupture zone. (a) An oblique UAV image of a rupture section along the southernmost part of the surface ruptures in Pangana basin; (b) coseismic fault scarps (indicated by red arrows) and pre-existing fault scarps (indicated by white arrows). North view, see the location in (a); (c) the fault plane (indicated by the two red arrows) disclosed on the southern wall of the trench excavated across the surface rupture (see the location in (a)); U1–U3 are young sediment units. Red arrows show the locations of the fault trace. See Figure 1 for locations.

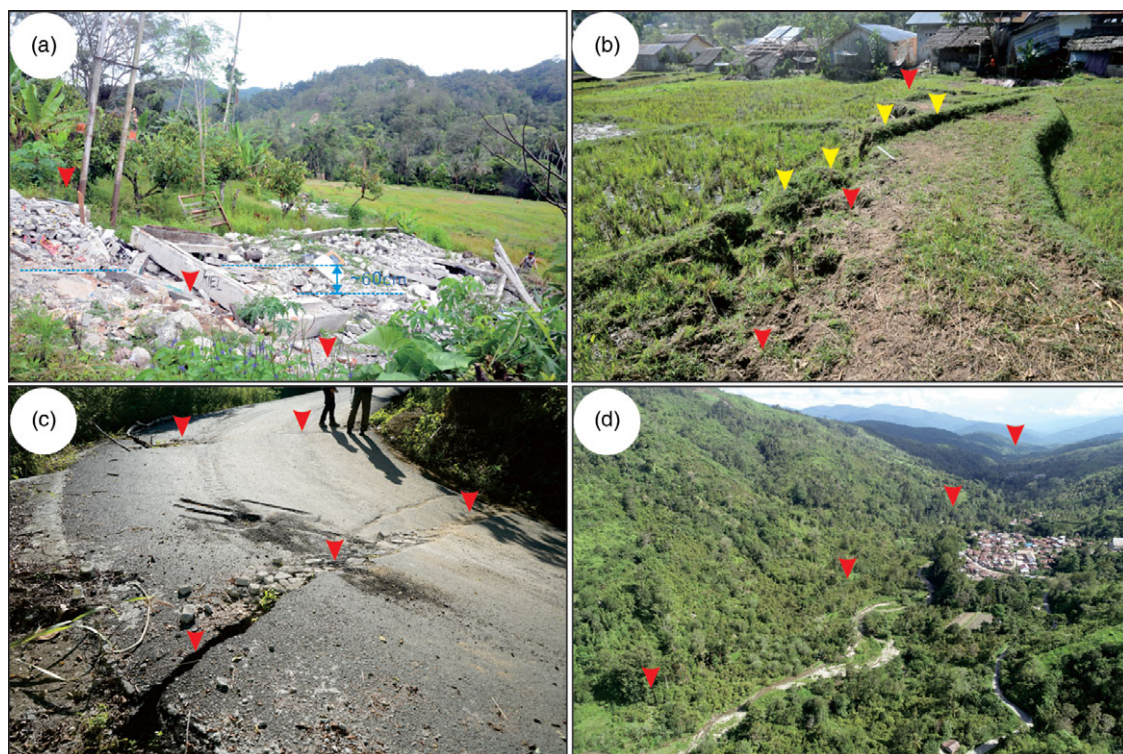


Fig. 7. (Colour online) Coseismic deformation along the southern segment of the surface rupture zone and tectonic geomorphology of the Palu–Koro fault south of the 2018 rupture. (a) A ~60 cm high fault scarp formed during the earthquake at the northern part of Pangana basin, view to the northeast. (b) The coseismic left-lateral and vertical displacements of the field edges close to the southern end of the rupture zone were ~50 cm and 40 cm, respectively (view is to the east). (c) Open cracks along the fault south of the Pangana basin, where the rupture terminated (south view); (d) the geomorphic expression of the fault that was not ruptured during the 2018 event (south view). Red arrows show the locations of the fault trace. See Figure 1 for locations.

earthquake ruptured a ~150 km long part of the Palu–Koro fault, and displayed a predominantly left-lateral strike-slip motion with some dip-slip component on the surface. The maximum strike-, normal and thrust slips are ~5.5 m, ~2 m and ~2 m, respectively.

4.a. The surface rupture zone of the 2018 event shows two unique features regarding a plate-boundary strike-slip fault

According to the field observations, two remarkable features characterize the 2018 surface ruptures. One is that the rupture was dominated by sinistral motions with a normal component in the middle segment, in contrast to thrust components in the northern and southern segments. This feature illustrates that the Palu–Koro fault acts as a transform fault connecting the two subduction zones in the north and south (Fig. 8a). The thrust components in the northern and southern parts are consistent with the shortening across them, which reflects a transpressional stress regime (Fig. 8a). Thrust slip on the northern part of the Palu–Koro fault has been documented by GPS results, which indicate an 8 mm a^{-1} shortening across the fault (Stevens *et al.* 1999). This thrust slip has also been observed in geological investigation, and can be considered as corresponding to an early (post-Oligocene stress) regime (Bellier *et al.* 2006). Reverse faulting in the southern part of the Palu valley has been observed for the first time in our fieldwork. Evidence from geomorphic expression and trench result is reasonable. These two segments act as transpressional structures that accommodate the present-day convergence of the Sula block with the Sunda plate in the north and with the Australian plate in the south (Fig. 8a). The normal faulting in the middle segment is related to an east-trending extension, suggesting that the transtensional regime corresponds to the fault activity in this area. It accommodates the relative motion between the Makassar block, which rotates anticlockwise, and the Sula block, which rotates clockwise (Socquet *et al.* 2006).

The second notable feature is that the middle segment (the Palu segment) exhibits an unusual geometry that consists of two distinct, roughly parallel strands showing almost pure strike-slip and normal faulting (Fig. 8b). Such an extraordinary structure can be explained by slip partitioning between coseismic strike-slip and normal faulting along an oblique slip fault zone. Coseismic oblique slip along a fault zone partitioned on two or more faults with different motions in a single event is rarely observed (King *et al.* 2005; Klinger *et al.* 2005). The same partitioning occurred during the 2001 Kunlun earthquake between coseismic strike-slip and normal faulting on two parallel fault strands along a 70 km long rupture segment (King *et al.* 2005). Previous studies have pursued a mechanism for slip partitioning (Bowman *et al.* 2003; King *et al.* 2005). Bowman *et al.* (2003) proposed that slip partitioning can be explained as a result of upward propagation of oblique shear at depth. King *et al.* (2005) suggested that the likely mechanical cause of such partitioning is the rupture travelling faster at depth than near the surface, leaving the surface deformation to catch up. The slip partition on the 2018 earthquake rupture corresponds to the faulting characteristics of the segment of the Palu–Koro fault as a transtensional structure.

4.b. Coseismic slip partitioning contributed much to the supershear speed

Consequently, the above-stated two focal issues of the 2018 earthquake rupture could possibly be resolved now by understanding the geometry and faulting characteristics of the rupture. One is that the Mw 7.5 earthquake may have ruptured at a supershear

speed, according to the results from seismic inversion, geodetic observations and joint analysis (Bao *et al.* 2019; Socquet *et al.* 2019; Ulrich *et al.* 2019). Our mapping of the surface rupture of the Mw 7.5 earthquake south of Palu bay shows that these two segments display a geometrically simple trace with linear, smooth, straight and narrow features, all of which are consistent with the typical geometric characteristics associated with supershear earthquakes (Bouchon *et al.* 2010). Through this unique scenario of coseismic slip partitioning along the middle segment, the vertical component is accommodated onto a secondary fault (Fig. 8b), which enables the main fault to rupture a simple, smooth segment with a pure strike-slip motion, thus making supershear propagation more likely. Furthermore, normal faulting marks an extension that can possibly lower the friction strength on the major fault plane, hence favouring supershear faulting. Although there is an 8 km long bend that may have prevented the rupture from propagating southward, the mature properties and simple geometry (e.g. narrow, straight) of the fault segment south of the bend enabled the rupture to propagate at a supershear velocity. In addition, a maximum left-lateral displacement of $5.5 \pm 0.1 \text{ m}$ during the Palu earthquake occurs on the middle segment, which encourages a condition to localize the supershear rupture propagation there. Only one of these three segments is the northern segment that does not show mature properties of geometrically simple, smooth structures. Studies of relations between earthquake slip and fault properties suggest that rupture speeds are controlled by the along-strike changes of fault maturity (Bruhat *et al.* 2016; Huang *et al.* 2016; Perrin *et al.* 2016). Rupture propagation speeds are faster along the most mature sections, while along the most immature sections ruptures travel at subshear velocities. From this point, conditions of the northern segment likely enabled only a subshear speed. Thus, the 2018 rupture might not have propagated at a supershear speed initially as argued by Bao *et al.* (2019), but only at a subshear speed in the northern segment, while in the middle and southern segments it propagated at a speed much faster than that which they proposed, 4.1 m s^{-1} .

4.c. The Palu earthquake tsunami is owed to a normal slip on the fault within Palu bay

The other issue is that the Mw 7.5 Palu earthquake generated a devastating tsunami, which is commonly associated with earthquakes occurring on thrust or reverse faults in subduction zones (Carvajal *et al.* 2018; Mikami *et al.* 2019; Omira *et al.* 2019; Ulrich *et al.* 2019). However, a strike-slip earthquake can also generate a tsunami when the submarine faulting has a component of vertical displacement, or when it triggers a landslide. The post-earthquake bathymetry within Palu bay defines a trans-tensional graben along the submarine channel that is indicated to be bounded by the Palu–Koro fault (Frederik *et al.* 2019). Based on the bathymetric data, no apparent evidence of recent slumping and lateral spreading was observed on the bay floor, suggesting that a submarine landslide as the cause of the tsunami can be excluded. Although the 2018 rupture was not clearly shown due to the limit resolution of the bathymetric data, a significant submarine normal faulting was observed in seismic and geodetic studies (Fang *et al.* 2019; Ulrich *et al.* 2019). As opposed to the viewpoint that dip-slip is the main cause of the tsunami, some researchers ascribe the tsunami to submarine landslides. Most proponents of the landslide-induced tsunami hypothesis obtained their results from numerical simulations based on data of remote-sensing images. Some studies indicate that tsunami waves were generated by coastal

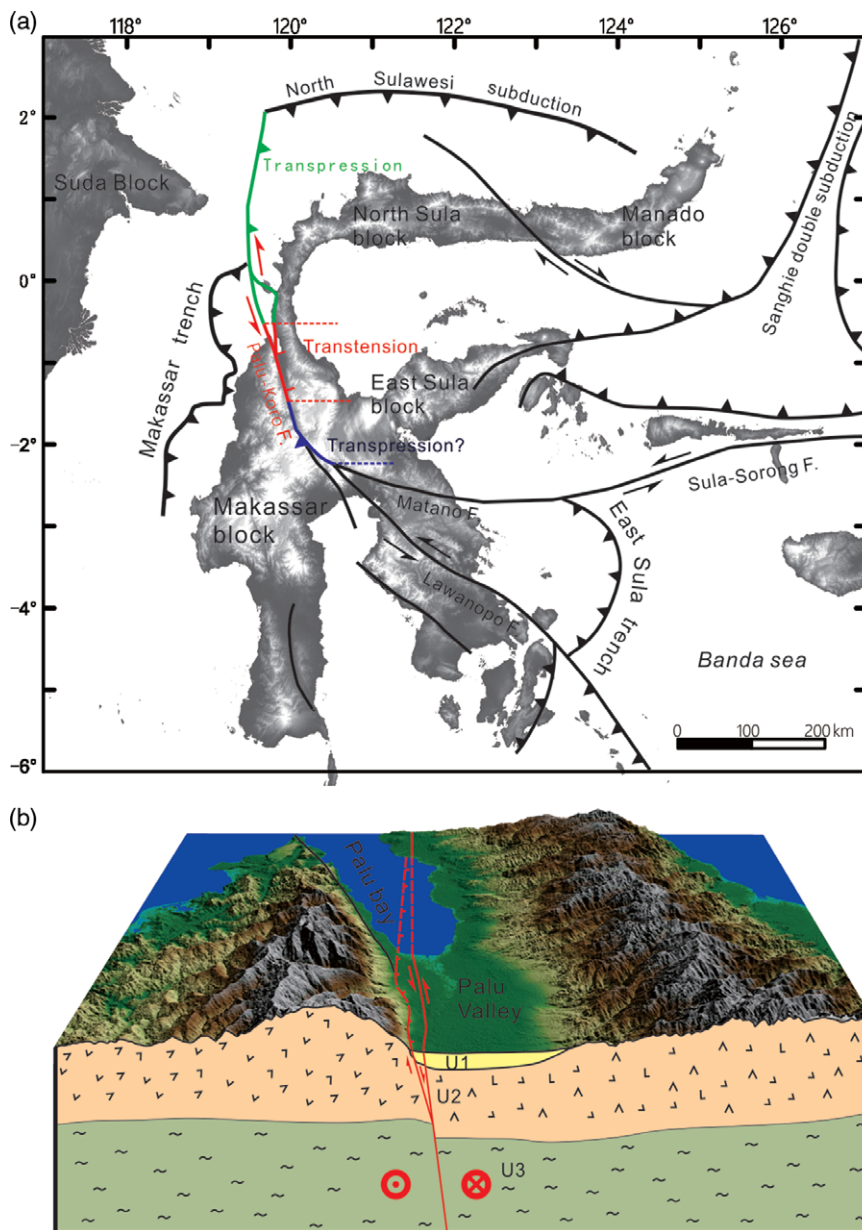


Fig. 8. (Colour online) (a) The mode of the Palu-Koro fault and the main faults surrounding the island of Sulawesi. The Palu-Koro fault behaves as a transform fault accommodating the collisions and rotation between different blocks. (b) A three-dimensional model of the Palu-Koro fault in the Palu valley. The two rupture strands are linked at depth. Cross-sections are constructed based on geological reports from Hamilton (1979) and Watkinson & Hall (2017). U1: Quaternary layers; U2: Cenozoic volcanics and rocks; U3: schist.

landslide sources (Takagi *et al.* 2019; Aránguiz *et al.* 2020); however, they cannot explain the tsunami-wave records (Liu *et al.* 2020). Detailed landslide simulations are unable to consider the physical model of a landslide tsunami in order to investigate the possibility of a submarine landslide source. Hence, they underestimate tsunami excitation due to underwater fault movements but solely attributed to massive underwater landslides. Coseismic deformation studies reveal a primarily horizontal strike-slip motion, with a vertical slip component of 1–3 m along the Palu bay section (e.g. Jamelot *et al.* 2019; Socquet *et al.* 2019; Yolsal-Çevikbilen & Taymaz 2019), suggesting a tectonic tsunami source. Our field investigation also suggests possible rupture on a normal fault strand in Palu bay, which is probably the continuation of the part observed in the Palu valley, and could have a similar expression. Our observations support the findings from seismic and geodetic data that a left-lateral strike slip of up to ~5.5 m with normal slip of up to ~2 m occurred along the fault part around Palu bay (Fang *et al.* 2019; Ulrich *et al.* 2019). Normal slip of the fault in Palu bay may have induced a large portion

of the tsunami waves, and those coastal landslides may make some contribution to the tsunami but not be the main tsunami source. Thus, we can speculate that the considerable normal slip favours tsunami genesis.

5. Conclusions

By mapping the surficial breaks through field investigations complemented with detailed analysis of high-resolution satellite images, we document geometric and geomorphic features of the surface ruptures of the Palu Mw 7.5 earthquake along the Palu-Koro fault. Our investigation shows that the fault exhibits a complex transforming behaviour, which demonstrates the features of the Palu-Koro fault as a strike-slip fault connecting subduction zones. The transtensive behaviour of the middle segment of the rupture, which contains a substantial normal slip, accounts for the generation of the large tsunami. Our results for the surface rupture geometry support the Palu earthquake as a supershear event.

Supplementary material. To view supplementary material for this article, please visit <https://doi.org/10.1017/S0016756822000012>

Acknowledgements. This study was funded by the National Nonprofit Fundamental Research Grant of China, IGCEA (IGCEA1901), the National Research and Development Program of China (2017YFC1500101) and the National Natural Science Foundation of China (42072250). We thank Professor Pavel Adamek (Nanyang Technological University) and Dr Murat Tamer for comments and English grammar corrections. We also thank editor Olivier Lacombe and anonymous reviewers for thoughtful comments that significantly improved the manuscript.

Declaration of Competing Interests. The authors declare no competing interests.

References

- Ammon CJ, Ji C, Thio HK, Robinson D, Ni SD, Hjorleifsdottir V, Kanamori H, Lay T, Das S, Helmlinger D, Ichinose G, Polet J and Wald D (2005) Rupture process of the 2004 Sumatra-Andaman earthquake. *Science* **308**, 1133–9.
- Aránguiz R, Esteban M, Takagi H, Mikami T, Takabatake T, Gómez M, González J, Shibayama T, Okuwaki R, Yagi Y, Shimizu K, Achiari H, Stolle J, Robertson I, Ohira K, Nakamura R, Nishida Y, Krautwald C, Goseberg N and Nistor I (2020) The 2018 Sulawesi tsunami in Palu city as a result of several landslides and coseismic tsunamis. *Coastal Engineering Journal* **62**, 445–59.
- Banerjee P, Pollitz F, Nagarajan B and Bürgmann R (2007) Coseismic slip distributions of the 26 December 2004 Sumatra-Andaman and 28 March 2005 Nias earthquakes from GPS static offsets. *Bulletin of the Seismological Society of America* **97**, S86–S102.
- Bao H, Ampuero JP, Meng L, Fielding EJ, Liang C, Milliner CW, Feng T and Huang H (2019) Early and persistent supershear rupture of the 2018 magnitude 7.5 Palu earthquake. *Nature Geoscience* **12**, 200–5.
- Bellier O, Sebrrier M, Beaudouin T, Villeneuve M, Braucher R, Bourlès D, Siame L, Putranto E and Pratomo I (2001) High slip rate for a low seismicity along the Palu-Koro active fault in central Sulawesi (Indonesia). *Terra Nova* **13**, 463–70.
- Bellier O, Sébrrier M, Seward D, Beaudouin T, Villeneuve M and Putranto E (2006) Fission track and fault kinematics analyses for new insight into the Late Cenozoic tectonic regime changes in West-Central Sulawesi (Indonesia). *Tectonophysics* **413**, 201–20.
- Bouchon M, Karabulut H, Bouin MP, Schmittbuhl J, Vallée M, Archuleta R, Das S, Renard F and Marsan D (2010) Faulting characteristics of supershear earthquakes. *Tectonophysics* **493**, 244–53.
- Bouchon M and Vallée M (2003) Observation of long supershear rupture during the magnitude 8.1 Kunlunshan earthquake. *Science* **301**, 824–6.
- Bowman D, King G and Tapponnier P (2003) Slip partitioning by elastoplastic propagation of oblique slip at depth. *Science* **300**, 1121–3.
- Bruhat L, Fang Z and Dunham EM (2016) Rupture complexity and the supershear transition on rough faults. *Journal of Geophysical Research* **121**, 210–24.
- Carvajal M, Araya-Cornejo C, Sepúlveda I, Melnick D and Haase JS (2018) Nearly instantaneous tsunamis following the Mw 7.5 2018 Palu earthquake. *Geophysical Research Letters* **46**, 5117–26. doi: [10.1029/2019gl082578](https://doi.org/10.1029/2019gl082578).
- Fang J, Xu CJ, Wen YM, Wang S, Xu GY, Zhao YW and Yi L (2019) The 2018 Mw 7.5 Palu earthquake: a supershear rupture event constrained by InSAR and Broadband regional seismograms. *Remote Sensing* **11**, 1330. doi: [10.3390/rs11111330](https://doi.org/10.3390/rs11111330).
- Fitch TJ (1972) Plate convergence, transcurrent faults and internal deformation adjacent to southeast Asia and the western Pacific. *Journal of Geophysical Research* **77**, 4432–60.
- Frederik MC, Adhitama R, Hananto ND, Sahabuddin S, Irfan M, Moefi O, Putra DB and Riyalda BF (2019) First results of a bathymetric survey of Palu Bay, Central Sulawesi, Indonesia following the Tsunamigenic Earthquake of 28 September 2018. *Pure and Applied Geophysics* **176**, 3277–90.
- Hamilton W (1979) Tectonics of the Indonesian Region. *US Geological Survey Professional Paper* 1078.
- Heidarzadeh M, Muhari A and Wijanarto AB (2019) Insights on the source of the 28 September 2018 Sulawesi tsunami, Indonesia based on spectral analyses and numerical simulations. *Pure and Applied Geophysics* **176**, 25–43.
- Huang Y, Ampuero JP and Helmlinger DV (2016) The potential for supershear earthquakes in damaged fault zones: theory and observations. *Earth and Planetary Science Letters* **433**, 109–15.
- Jamelot A, Gailler A, Heinrich P, Vallage A and Champenois J (2019) Tsunami simulations of the Sulawesi Mw 7.5 event: comparison of seismic sources issued from a tsunami warning context versus post-event finite source. *Pure and Applied Geophysics* **176**, 3351–76.
- King G, Klinger Y, Bowman D and Tapponnier P (2005) Slip partitioned surface breaks for the 2001 Kokoxili earthquake, China (Mw 7.8). *Bulletin of the Seismological Society of America* **95**, 731–8.
- Klinger Y, Xu X, Tapponnier P, Van der Woerd J, Lasserre C and King G (2005) High-resolution satellite imagery mapping of the surface rupture and slip distribution of the Mw 7.8, 14 November 2001 Kokoxili earthquake, Kunlun fault, northern Tibet, China. *Bulletin of the Seismological Society of America* **95**, 1970–87.
- Konca AO, Leprince S, Avouac JP and Helmlinger DV (2010) Rupture process of 2010, Mw= 7.1 Düzce earthquake from joint analysis of SPOT, GPS, InSAR, strong-motion and teleseismic data: a super-shear rupture with variable rupture velocity. *Bulletin of the Seismological Society of America* **100**, 267–88.
- Kreemer C, Holt WE, Goes S and Govers R (2000) Active deformation in eastern Indonesia and the Philippines from GPS and seismicity data. *Journal of Geophysical Research* **105**, 663–80.
- Li Q, Zhao B, Tan K and Xu W (2020) Two main rupture stages during the 2018 magnitude 7.5 Sulawesi earthquake. *Geophysical Journal International* **221**, 1873–82.
- Liu P, Higuera P, Husrin S, Prasetya G, Prihantono J and Diastomo H (2020) Coastal landslides in Palu Bay during 2018 Sulawesi earthquake and tsunami. *Landslides* **17**, 2085–98.
- Mikami T, Shibayama T, Esteban M, Takabatake T, Nakamura R, Nishida Y, Achiari H, Rusli Marzuki AG, Marzuki MFH, Stolle J, Krautwald C, Robertson I, Aránguiz R and Ohira K (2019) Field survey of the 2018 Sulawesi tsunami: inundation and run-up heights and damage to coastal communities. *Pure and Applied Geophysics* **176**, 3291–304.
- Omira R, Dogan GG, Hidayat R, Husrin S, Prasetya GS, Annunziato A, Proietti C, Probst P, Paparo MA, Wronna M, Zaytsev A, Pronin PI, Giniyatullin AA, Putra PS, Hartanto D, Ginanjar G, Kongko W, Pelinovsky EN and Yalciner AC (2019) The September 28th, 2018, tsunami in Palu-Sulawesi, Indonesia: a post-event field survey. *Pure and Applied Geophysics* **176**, 1379–95.
- Perrin C, Manighetti I, Ampuero JP, Cappa F and Gaudemer Y (2016) Location of largest earthquake slip and fast rupture controlled by along-strike change in fault structural maturity due to fault growth. *Journal of Geophysical Research* **121**, 3666–85.
- Prasetya GS, De Lange WP and Healy TR (2001) The Makassar strait tsunamigenic region, Indonesia. *Natural Hazards* **24**, 295–307.
- Rangin C, Le Pichon X, Mazzotti S, Pubellier M, Chamot-Rooke N, Aurelio M, Walpersdorf A and Quebral R (1999) Plate convergence measured by GPS across the Sundaland/Philippine Sea plate deformed boundary: the Philippines and eastern Indonesia. *Geophysical Journal International* **139**, 296–316.
- Silver EA, McCaffrey R and Smith RB (1983) Collision, rotation and the initiation of subduction in the evolution of Sulawesi, Indonesia. *Journal of Geophysical Research* **88**, 9407–18.
- Socquet A, Hollingsworth J, Pathier E and Bouchon M (2019) Evidence of supershear during the 2018 magnitude 7.5 Palu earthquake from space geodesy. *Nature Geoscience* **12**, 192–99.
- Socquet A, Simons W, Vigny C, McCaffrey R, Subarya C, Sarsito D, Ambrosius B and Spakman W (2006) Microblock rotations and fault coupling in SE Asia triple junction (Sulawesi, Indonesia) from GPS and earthquake slip vector data. *Journal of Geophysical Research Solid Earth* **111**, B08409. doi: [10.1029/2005JB003963](https://doi.org/10.1029/2005JB003963).
- Stevens C, McCaffrey R, Bock Y, Genrich J, Endang, Subarya C, Puntodewo SSO, Fauzi and Vigny C (1999) Rapid rotations about a vertical axis in a

- collisional setting revealed by the Palu fault, Sulawesi, Indonesia. *Geophysical Research Letters* **26**, 2677–80.
- Subarya C, Chlieh M, Prawirodirdjo L, Avouac JP, Bock Y, Sieh K, Meltzner AJ, Natawidjaja DH and McCaffrey R** (2006) Plate boundary deformation associated with the great Sumatra-Andaman earthquake. *Nature* **440**, 46–51.
- Surmont J, Laj C, Kisse, C, Rangin C, Bellon H and Priadi B** (1994) New paleomagnetic constraints on the Cenozoic tectonic evolution of the North Arm of Sulawesi, Indonesia. *Earth and Planetary Science Letters* **121**, 629–38.
- Takagi H, Pratama M, Kurobe S, Esteban M, Aránguiz R and Ke B** (2019) Analysis of generation and arrival time of landslide tsunami to Palu city due to the 2018 Sulawesi earthquake. *Landslides* **16**, 983–91.
- Titov V, Rabinovich AB, Mofjeld HO, Thomson RE and Gonzalez FI** (2005) The global reach of the 26 December 2004 Sumatra tsunami. *Science* **309**, 2045–8.
- Ulrich T, Vater S, Madden EH, Behrens J, Van Dinther Y, Van Zelst I, Fielding E, Liang C and Gabriel A** (2019) Coupled, physics-based modeling reveals earthquake displacements are critical to the 2018 Palu, Sulawesi Tsunami. *Pure and Applied Geophysics* **176**, 4069–109.
- US Geological Survey (USGS)** (2018) M7.5-7.2 km N of Palu, Indonesia (usgs.gov). <https://earthquake.usgs.gov/earthquakes/eventpage/us1000h3p4/moment-tensor> (Accessed 1 February 2022).
- Vallée M, Landès M, Shapiro NM and Klinger Y** (2008) The 14 November 2001 Kokoxili (Tibet) earthquake: high frequency seismic radiation originating from the transition between sub-Rayleigh and supershear rupture velocity regimes. *Journal of Geophysical Research* **113**, B07305. doi: [10.1029/2007JB005520](https://doi.org/10.1029/2007JB005520).
- Vigny C, Perfettini H, Walpersdorf A, Lemoine A, Simons W, van Loon D, Ambrosius B, Stevens C, Mc Caffrey R, Morgan P, Bock Y, Subarya C, Manurung P, Kahar J, Abidin H and Abu S** (2002) Migration of seismicity and earthquake interactions monitored by GPS in SE Asia triple junction: Sulawesi, Indonesia. *Journal of Geophysical Research* **107**, 2231. doi: [10.1029/2001JB000377](https://doi.org/10.1029/2001JB000377).
- Vigny C, Simons WJF, Abu S, Bamphenyu R, Satirapod C, Choosakul N, Subarya C, Socquet A, Omar K, Abidin HZ and Ambrosius BAC** (2005) Insight into the 2004 Sumatra-Andaman earthquake from GPS measurements in southeast Asia. *Nature* **436**, 201–6.
- Walpersdorf A, Rangin C and Vigny C** (1998a) GPS compared to long-term geologic motion of the north arm of Sulawesi. *Earth and Planetary Science Letters* **159**, 47–55.
- Walpersdorf A, Vigny C, Subarya C and Manurung P** (1998b) Monitoring of the Palu-Koro Fault (Sulawesi) by GPS. *Geophysical Research Letters* **25**, 2313–6.
- Watkinson IM and Hall R** (2017) Fault systems of the eastern Indonesian triple junction: evaluation of Quaternary activity and implications for seismic hazards. In *Geohazards in Indonesia: Earth Science for Disaster Risk Reduction* (eds PR Cummins and I Mellano), pp. 71–120. *Geological Society of London, Special Publication* no. **441**.
- Wu D, Ren Z, Liu J, Chen J, Guo P, Yin G, Ran H, Li C and Yang X** (2020) Coseismic surface rupture during the 2018 Mw 7.5 Palu earthquake, Sulawesi Island, Indonesia. *GSA Bulletin* **133**, 1157–66. doi: [10.1130/B35597.1](https://doi.org/10.1130/B35597.1).
- Yolsal-Çevikbilen S and Taymaz T** (2019) Source characteristics of the 28 September 2018 Mw 7.5 Palu-Sulawesi, Indonesia (SE Asia) earthquake based on inversion of teleseismic bodywaves. *Pure and Applied Geophysics* **176**, 4111–26.
- Zhang Y, Chen YT and Feng W** (2019) Complex multiple-segment ruptures of the 28 September 2018, Sulawesi, Indonesia, earthquake. *Science Bulletin* **64**, 650–2.